THERMAL REACTIONS OF OXYGEN ATOMS WITH ALKENES AT LOW TEMPERATURES ON INTERSTELLAR DUST

MICHAEL D. WARD AND STEPHEN D. PRICE[1]
Department of Chemistry, University College London, 20 Gordon Street, London WC1H 0AJ, UK; Michael.Ward@ucl.ac.uk, s.d.price@ucl.ac.uk

ABSTRACT

Laboratory experiments show that the thermal heterogeneous reactions of oxygen atoms may contribute to the synthesis of epoxides in interstellar clouds. The data set also indicates that the contribution of these pathways to epoxide formation, in comparison to non-thermal routes, is likely to be strongly temperature dependent. Our results indicate that an increased abundance of epoxides, relative to the corresponding aldehydes, could be an observational signature of a significant contribution to molecular oxidation via thermal O atom reactions with alkenes. Specifically surface science experiments show that both C_2H_4O and C_3H_6O are readily formed from reactions of ethene and propene molecules with thermalized oxygen atoms at temperatures in the range of 12–90 K. It is clear from our experiments that these reactions, on a graphite surface, proceed with significantly reduced reaction barriers compared with those operating in the gas phase. For both the C_2H_4 + O and the C_3H_6 + O reactions, the surface reaction barriers we determine are reduced by approximately an order of magnitude compared with the barriers in the gas phase. The modeling of our experimental results, which determines these reaction barriers, also extracts desorption energies and rate coefficients for the title reactions. Our results clearly show that the major product from the O + C_2H_4 reaction is ethylene oxide, an epoxide.

Key words: astrochemistry – ISM: clouds – ISM: molecules

1. INTRODUCTION

The composition of the interstellar medium (ISM) is dominated by hydrogen and helium with carbon, oxygen, and nitrogen being 4 or 5 orders of magnitude less abundant than hydrogen (Herbst 1995). These fundamental chemical building blocks are not uniformly distributed across interstellar space but aggregate in a variety of interstellar environments such as diffuse and dense interstellar clouds (Hartquist 1990; Snow & McCall 2006; Tielens 2005). In these interstellar clouds, atoms and molecules are accompanied by dust grains of sizes comparable with the wavelengths of visible light, these grains making up about 1% of the mass of the clouds (Williams & Herbst 2002). Despite the overwhelming abundance of hydrogen, interstellar clouds have a rich, complex, and widely speciated chemistry, as evidenced by the over 150 molecules detected to date in the ISM (Burke & Brown; Lattelais et al. 2010). The abundances of many of these interstellar molecules cannot be explained solely by chemical synthesis in the gas phase, and it is now widely accepted that reactions at the surfaces of interstellar dust grains play an important role in the formation mechanisms of many interstellar molecules (see Burke & Brown; Cuppen & Herbst 2007; Tielens 2005; Williams & Hartquist 1999; Williams & Herbst 2002, and references therein). However, due to the low temperatures of interstellar dust grains (typically 10 K; Snow & McCall 2006) chemical reactions of thermalized surface species, so-called thermal synthetic routes, can only proceed via pathways with very low or non-existent reaction barriers.

An alternative to thermal processes, for the synthesis of molecules on grain surfaces, involves the energetic processing of the molecules in the icy mantles which accumulate on the dust grains in the cooler interstellar clouds (Williams & Herbst 2002). This processing of the molecular ices can occur via their interaction with ultraviolet photons and cosmic rays (Garozzo et al. 2011). This irradiation allows the generation of energized species within the ices, which are sufficiently energetic to overcome reaction barriers. These "non-thermal" reaction pathways have been invoked to explain the abundance of a wide variety of interstellar molecules from OCS to larger organic molecules such as ethanol (Ferrante et al. 2008; Garozzo et al. 2010; Hudson & Moore 1997; Schriver et al. 2007). Indeed, the interstellar formation of the reactant hydrocarbon molecules involved in the experiments reported in this paper, ethene (C_2H_4) and propene (C_3H_6), has been attributed to the energetic processing of icy mantles containing small hydrocarbons such as methane (Bennett et al. 2006; Kaiser & Roessler 1998).

At low temperatures on surfaces, the interaction of O atoms and ethene could be expected to form products of chemical formula C_2H_4O. These products can be generated in three isomeric forms (Figure 1): ethylene oxide (I), acetaldehyde (II), and vinyl alcohol (III). All three of these C_2H_4O isomers have been detected in the ISM. Acetaldehyde has been observed in translucent clouds (Turner et al. 1999), cold molecular clouds (Matthews et al. 1985; Turner et al. 1999), and star-forming regions (Bell et al. 1983; Charnley 2004; Fourikis et al. 1974; Ikeda et al. 2001; Nummelin et al. 1998; Turner 1991; Ziurys & McGonagle 1993). Ethylene oxide has been detected toward hot cores (Dickens et al. 1997; Ikeda et al. 2001; Nummelin et al. 1998) and has recently been proposed as a carrier of the unidentified infrared bands (Bernstein & Lynch 2009). Vinyl alcohol has been observed in the hot core Sgr B2N (Turner & Apponi 2001), a source in which all three of the C_2H_4O isomers have been identified.

As recently discussed (Bennett et al. 2005), a variety of mechanisms have been put forward for the formation of gas-phase acetaldehyde, ethylene oxide, and vinyl alcohol in the ISM. Consideration of these mechanisms, involving both ion–molecule and neutral–neutral chemistry, leads Charnley (2004) to conclude that such gas-phase pathways are not a major route to acetaldehyde and its isomers in star-forming regions. The

---

[1] Author to whom correspondence should be addressed.
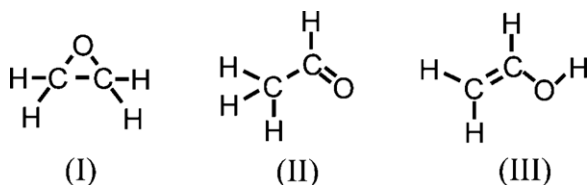
Figure 1. Possible isomeric forms of the C_2H_4O product from the reaction of O atoms with C_2H_4.

obvious alternative pathways for C_2H_4O synthesis involve reactions on dust grain surfaces. A possible series of thermal pathways for synthesis of acetaldehyde have been presented (Charnley 2004, and references therein) and such pathways have been shown to account for some observational characteristics of large O-bearing organic molecules in star-forming regions.

Non-thermal processing of ices to form acetaldehyde and its isomers has been investigated experimentally under conditions relevant to the ISM (Bennett et al. 2005; Hawkins & Andrews 1983; Hudson & Moore 2003). An early study of the C_2H_4 + O reaction involved irradiating a mixed ozone/C_2H_4 ice, deposited at 15–20 K, with UV–visible photons (Hawkins & Andrews 1983). Under these conditions the O_3 was photolyzed to produce "hot" O atoms which then reacted with adjacent C_2H_4 molecules in the ice. Infrared spectroscopy of the irradiated ices confirmed the formation of acetaldehyde, ethylene oxide, vinyl alcohol, and ketene (H_2CCO). In 2003, a study of the UV and proton irradiation of H_2O/C_2H_2 ices was shown to generate vinyl alcohol (Hudson & Moore 2003). The formation of the three C_2H_4O isomers following electron irradiation of mixed CO_2/C_2H_4 ices has also been investigated in great detail, the electron irradiation mimicking the electronic energy transfer processes occurring in the tracks of cosmic rays through astrophysical ices (Bennett et al. 2005). Product detection, again using infrared spectroscopy, indicates supra-thermal oxygen atoms, generated from CO_2 by the incident electrons, readily react with ethene. These interactions form ethylene oxide, by direct addition, and acetaldehyde via an oxirane intermediate; a minor channel involving insertion into a C–H bond to form vinyl alcohol was also observed.

The above studies of the reaction of C_2H_4 with supra-thermal O atoms under astrophysically relevant conditions demonstrate that the three C_2H_4O isomers can be formed via non-thermal chemistry in mixed ices. However, such investigations can only offer restricted information on the kinetics and energetics of the surface reaction. For example, as noted before (Bennett et al. 2005), it is not possible to derive a reaction barrier from such supra-thermal studies, since the energy distribution of the reacting oxygen atom is not well characterized.

To date, no studies of the surface reactivity between C_2H_4 and *thermal* O atoms have been carried out under astrophysically relevant conditions. The absence of such studies has perhaps stemmed from an assumption that the significant reaction barrier to this reaction in the gas phase (Atkinson & Cvetanov 1972; Perry 1984) would preclude such a surface reaction having any astrophysical importance. However, recent computational investigations have shown that atom + molecule reactions on model interstellar grain surfaces may proceed via pathways involving markedly lower barriers than those that have to be traversed in the gas phase (Adriaens et al. 2010). Thus, given the notable absence of an O + C_2H_4 pathway in the proposed thermal synthetic schemes for the formation of C_2H_4O on interstellar surfaces (Charnley 2004), we decided to investigate this heterogeneous reaction under thermalized and astrophysically relevant conditions.

Experimentally confirming that the surface reaction has a markedly lower barrier than in the gas phase, we report in this paper observations that thermal O atoms react readily with C_2H_4 to form C_2H_4O, on a highly oriented pyrolitic graphite (HOPG) surface, at a range of temperatures down to 20 K. Modeling our experimental results allows us to extract the activation energies for the surface reactions which are shown to be dramatically reduced in comparison with those controlling the gas-phase reactivity. Using a novel laser ionization methodology we have been able to identify the major product of the thermal C_2H_4 + O reaction as being ethylene oxide accompanied by some acetaldehyde. These observations indicate that thermal routes for ethylene oxide and acetaldehyde formation are available on interstellar dust grains.

We have also extended these studies to investigate the reaction of O atoms with propene (C_3H_6) on HOPG at interstellar temperatures. This reaction has also been widely studied in the gas phase (see, for example, Atkinson & Cvetanov 1972; Atkinson & Pitts 1974; Knyazev et al. 1992; Perry 1984; Stuhl & Niki 1971). However, to our knowledge no prior studies of this reaction on a surface have been carried out under astrophysically relevant conditions. Propene has been recently observed in TMC-1, and the formation of such small hydrocarbons via hydrogenation on grain surfaces has been postulated (Marcelino et al. 2007). However, recent calculations of radiative association rates indicate that gas-phase routes to propene are viable in dense clouds (Herbst et al. 2010). Similarly to the reaction of O with C_2H_4, our experiments show that O atoms react efficiently with C_3H_6 on HOPG at astrophysical temperatures to generate C_3H_6O.

2. EXPERIMENTAL

The experimental apparatus employed in this study has been previously used for the investigation of the formation of molecular hydrogen on interstellar surfaces and has been extensively described in the literature; only the salient experimental changes are given below (Islam et al. 2007; Latimer et al. 2008; Perry et al. 2002). In brief, two sources allow the dosing of radicals and stable molecules onto a cooled HOPG surface. Molecules formed on the surface as a result of this dosing can be detected and identified, using mass spectrometry or laser spectroscopy, in a subsequent temperature-programmed desorption experiment.

The experiment is housed in two differentially pumped stainless steel vacuum chambers. Two identical microwave discharge cells are installed in a high-vacuum "source" chamber, while a second ultra high vacuum "target" chamber contains a cryogenically cooled HOPG substrate mounted adjacent to the source region of a time-of-flight mass spectrometer (TOFMS). The base pressure in the source chamber is typically 1×10^{-7} Torr, while in the target chamber the base pressure is 1×10^{-10} Torr. Gases from the microwave discharge cells are transported to the target surface via PTFE tubes (Wise & Wood 1967). Using the TOFMS, the molecules desorbing from the HOPG surface, as its temperature is raised, can be identified by ionizing them with either an electron beam or a wavelength-selected laser beam.

The two gas lines which transport the reactants to the target surface each consist of two lengths of PTFE tubing connected in the source chamber via a PTFE connector which allows differential pumping. This differential pumping results in most of the gas from the microwave discharge cells being pumped

away via the source chamber allowing sufficient pressure of gas to be maintained in the microwave discharge cells for stable operation, while maintaining a low pressure in the target chamber. Microwaves can be supplied to both discharge cells or to either cell individually. We thus have the facility for co-depositing two separate species onto the HOPG substrate which may either be stable gas-phase molecules or radical species produced from a discharge. In the current experiments, we co-deposit oxygen atoms (O) produced from a microwave discharge in molecular oxygen (O_2), along with a pure sample of the relevant alkene (either ethene or propene). The dissociation efficiency of O_2 gas in the microwave discharge was measured via electron ionization of the gas directly effusing from the PTFE tube. At the microwave discharge pressure (0.2 Torr) used in the present experiments the dissociation efficiency was found to be approximately 20%, resulting in a 2:1 mixture of molecular and atomic oxygen in the oxygen beam. The ratio of the fluxes of C_nH_{2n} and (O + O_2) used for deposition in the present experiments was approximately 5:1, resulting in a C_nH_{2n}:O ratio of 10:1 during dosing. It should be noted that using O_2 as the precursor gas for O atom production does have a disadvantage in that residual O_2 deposited onto the substrate can combine with O atoms to form ozone. To alleviate this problem alternative precursor gases, particularly N_2O, are often used in order to generate O atoms to minimize O_2 contamination (Hiraoka et al. 1998; Ung 1975). However, the use of N_2O as a precursor gas in the current experiments is not possible as N_2O^+ ions would appear at the same m/z in the TOF mass spectra as any ionized C_2H_4O products, making the definitive detection of any reaction products very difficult. Furthermore, even with a discharge in N_2O, the recombination of O atoms within the PTFE transport tubes would mean that some O_2 would arrive at the HOPG surface. In our experiments we do see some ozone desorption following dosing at low surface temperatures. However, the observation of C_2H_4O products at higher temperatures (above 30 K), where ozone either does not form or does not remain on the surface, indicates that the products we observe do not result from the reaction of alkenes with ozone. This conclusion, that the trace quantities of O_3 do not influence our experimental results, is confirmed by the fact that in experiments studying reactivity in O_3/C_2H_4 matrices C_2H_4O formation only occurs following irradiation of the matrix (Hawkins & Andrews 1983).

A microwave discharge in O_2 may also produce electronically excited O ^1D atoms. However, we can be sure that any contribution to our results from the reaction of O ^1D with the alkenes is negligible since such a reaction would be expected to proceed at our very lowest surface temperature (12 K) where we see markedly reduced product formation. This conclusion is supported, in a separate experiment, by moving the laser beam to allow resonance-enhanced (2 + 1) laser ionization of the O(^3P) atoms in the O atom beam via the $2s^2 2p^3 3p$ (^3P) state. The O^+ signals in these laser ionization experiments are so large that again we conclude that O(^3P) species must be the dominant component in the O atom beam. Given the above observations, we conclude that any O(^1D) oxygen atoms formed in the discharge relax via interactions with either the walls of the PTFE tube or the oxygen molecules in the gas flow.

The HOPG target surface is mounted on the surface of a hollow copper block which houses a tantalum strip heater held between two pieces of insulating aluminum nitride. This copper block is in thermal contact with the cold head of a closed-cycle helium cryostat. The temperature of the HOPG substrate can be controlled in the range from 12 to 500 K by passing a current through the tantalum strip heater while the cold head is running.

In the present experiments, C_2H_4 and O or C_3H_6 and O were co-deposited onto the HOPG substrate at various substrate temperatures in the range from 12 to 90 K for 60 minutes in each experiment. Following the deposition of C_2H_4 (C_3H_6) and O onto the HOPG surface, the supply of both reactants was turned off and the HOPG substrate allowed to cool to 12 K. A current was then passed through the tantalum strip heater to warm the surface from 12 to 200 K, a temperature at which all the relevant species have desorbed. Species desorbing from the HOPG surface pass across the source region of the TOFMS where, in the standard experiments, they are ionized by 400 eV electrons from a pulsed electron gun (29 kHz). Following each pulse of electrons, the times of flight of the ions reaching the detector of the mass spectrometer are added to a histogram to give a mass spectrum. During the heating of the HOPG surface multiple short duration (1 s) mass spectra are recorded consecutively, generating a data set which is a two-dimensional histogram of ion intensity as a function of ion m/z ratio and surface temperature. One-dimensional desorption spectra of ion counts at a particular m/z ratio against temperature can be extracted from this two-dimensional data set. As summarized above, these desorption spectra clearly show the formation of C_2H_4O and C_3H_6O, from the reaction of O atoms with C_2H_4 and C_3H_6, at temperatures below 70 K and 90 K, respectively. The total counts in the desorption spectrum for the oxygenated product give the yield of C_2H_4O (C_3H_6O) when dosing the HOPG at a given surface temperature.

To identify the isomeric form (Figure 1) of the C_2H_4O product, separate experiments were carried out using the doubled output of a tunable dye laser (Coumarin 480) pumped by the frequency tripled light of an Nd:YAG laser (10 Hz) to ionize the reaction products desorbing from the surface during warming (Islam et al. 2007). The tunability of the laser photons allows us to selectively ionize the three different isomers (Figure 1) of C_2H_4O using two-photon ionization. The ionization energies of vinyl alcohol, acetaldehyde, and ethylene oxide are 9.33 eV, 10.23 eV, and 10.56 eV, respectively (Lias 2011). Thus, by setting the wavelength of the dye laser such that the two-photon energy was slightly above each of these ionization energies, we can ionize only vinyl alcohol, vinyl alcohol and acetaldehyde, or all three isomers, respectively. This methodology allows us to determine which isomers are formed from the thermal C_2H_4 + O reaction. The ionizing wavelengths used in these experiments were 245.0 nm (ionizes just vinyl alcohol), 240.0 nm (ionizes vinyl alcohol and acetaldehyde), and 234.0 nm (ionizes all three isomers). Given the low laser power used in these experiments (0.6 mJ pulse^{-1}) any contribution to the ion signal from three-photon ionization is negligible. Indeed, in separate experiments, the acetaldehyde and ethylene oxide isomers were separately admitted into the target chamber and laser ionization mass spectra recorded to confirm the specific ionization of the expected molecules at the above wavelengths. The laser ionization experiments were carried out in a similar way to the electron ionization experiments, after dosing for an hour at a surface temperature of 40 K, a temperature at which a good product yield is observed. Following deposition of the reactants, consecutive laser ionization mass spectra were taken while the surface was warmed to approximately 200 K. In the case of the laser ionization experiments the duration of each consecutive mass spectrum was longer (10 s) than for the electron ionization experiments in order to compensate for the markedly lower laser pulse rep-
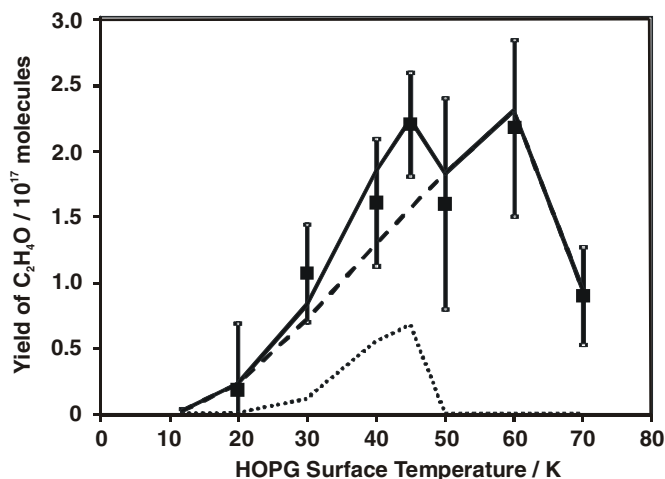
Figure 2. Temperature dependence of the yield of C_2H_4O molecules following co-deposition of C_2H_4 and O atoms for 1 hr. Squares: experiment; solid line: model; dashed line: ER mechanism; and dotted line: LH mechanism.

Figure 3. Temperature dependence of the yield of C_3H_6O molecules following co-deposition of C_3H_6 and O atoms for 1 hr. Squares: experiment; solid line: model; dashed line: ER mechanism; and dotted line: LH mechanism.

etition rate (10 Hz) in comparison with the electron gun (29 kHz).

Before embarking on the data acquisition for the reactions of the O atoms, baseline experiments were carried out in which the relevant alkene was deposited onto the surface together with pure O_2 gas (microwaves off in the O atom source). These experiments confirmed that no formation of oxygenated products occurred in the absence of O atoms.

3. RESULTS

3.1. $C_2H_4 + O$

The dependence of the yield of the C_2H_4O product, from the reaction of O with C_2H_4, on the temperature of the HOPG surface during dosing is shown in Figure 2. The product yield increases from 12 K, reaching a peak at 45 K. The product yield appears to decrease somewhat at 50 K before reaching a second peak at 60 K. Finally the product yield drops off rapidly above 60 K, with the yield at 70 K being less than half of that at 60 K. As discussed below, the unambiguous double peak observed in the yield of C_3H_6O from the reaction with propane, as well as the predictions of our model, strongly suggests that the double peak in Figure 2 is a real feature.

As outlined in Section 2, we have also conducted photoion-ization experiments at wavelengths of 245.0 nm (equivalent to a two-photon energy of 10.13 eV), 240.0 nm (10.34 eV), and 234.0 nm (10.61 eV) in order to determine the identity of the C_2H_4O product from the reaction of O with C_2H_4. We observe no ionized products at 245.0 nm indicating that no vinyl al-cohol is formed in our experiments. At 240.0 nm we observe a small but clear peak at m/z 44 which must be due to ac-etaldehyde while at 234.0 nm we observe a much larger peak at m/z 44 indicating that the majority of the C_2H_4O formed is the ethylene oxide isomer. This association of the yields of product photoions to the relative abundance of the different isomers of C_2H_4O relies on the fact that no resonant ionization is occur-ring at 234.0 nm. Such resonant ionization would dramatically enhance the ionization of acetaldehyde at this wavelength, a sig-nal which would then be interpreted as ethylene oxide. We have confirmed the absence of any such resonant enhancement by recording photoionization spectra of acetaldehyde and ethylene oxide independently. These experiments show the ion yield from
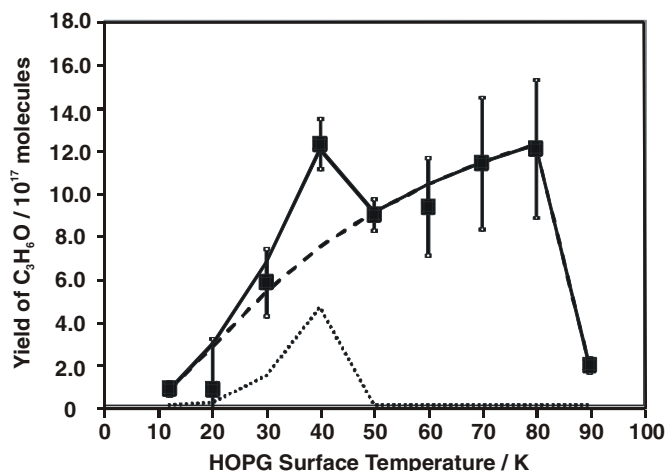
ionization of acetaldehyde is similar at 240.0 nm and 234.0 nm and that ethylene oxide is only ionized at 234.0 nm.

3.2. $C_3H_6 + O$

C_3H_6 dosed onto the HOPG surface was found to react with oxygen atoms to form C_3H_6O under astrophysically relevant conditions. The yield of this reaction as a function of surface temperature is shown in Figure 3. As with the reaction of O atoms with C_2H_4, the product yield generally increases with increasing surface temperature up to 80 K, before decreasing at higher temperatures. However, this trend is interrupted by a peak at 40 K which reaches approximately the same value as the peak at 80 K.

Unfortunately, the number of possible isomers of C_3H_6O make laser ionization experiments to identify the structure of the product molecule impractical. However, by analogy with the $C_2H_4 + O$ reaction, it seems reasonable to suggest that the major product is likely to be propylene oxide.

4. DATA REDUCTION

As described above, our experimental data set is processed to give the yield of oxygenated product (C_2H_4O or C_3H_6O) as a function of the surface temperature during the dosing (Figures 2 and 3). To account for these experimental data we have developed a simple kinetic model which allows us to quan-tify the surface processes occurring during our experiments. To establish this model we note that the reaction of the tar-get alkenes with oxygen atoms on the HOPG surface can oc-cur via two prototypical mechanisms: Eley–Rideal (ER) and Langmuir–Hinshelwood (LH).

In the ER mechanism a species from the gas phase $X(g)$ reacts with an adsorbed partner $Y(ads)$ without thermally equilibrating with the surface:

$$X(g) + Y(ads) \rightarrow XY(ads).$$
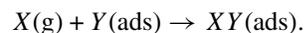
In the LH mechanism both reactants adsorb and thermalize on the surface, before diffusing to a mutual encounter and reacting:

$$X(ads) + Y(ads) \rightarrow XY(ads).$$

Our kinetic model involves calculating the rate of the above reactions, at a given surface temperature, throughout the dosing

period and integrating these rates to determine the total number of product molecules generated during the dosing period. This total number of product molecules can then be compared with the experimental product yield as a function of the surface temperature during the dosing. For our model we start with the rate equations for both the ER mechanism (Equation (1)) and the LH mechanism (Equation (2)) (Harris & Kasemo 1981):

$$r_{ER} = k_{ER}[X]_S F_Y \qquad (1)$$

$$r_{LH} = k_{LH}[X]_S [Y]_S, \qquad (2)$$

where r is the rate of reaction, $[X]_S$ and $[Y]_S$ are the number of species adsorbed on the HOPG surface per unit area and F_Y is the fluence of Y molecules onto the surface. Note that in our experiments, due to the low surface temperature and the consequent dominance of physisorption, the number of accessible surface sites is not in reality restricted as the reaction proceeds, as it is often in systems when chemisorption to the surface dominates the dynamics. As the graphite surface is filled with physisorbed reactants, and products, further molecules can be physisorbed in multi-layers, on top of the previous adsorbates. This operation in the physisorption regime means that an adsorption site is always available for an incoming molecule. Further nuances of surface chemistry in this regime are discussed below. The rate constants for the LH and ER reaction pathways are k_i (i = ER or LH), given by an Arrhenius expression:

$$k_i = A_i \exp\left(\frac{-E_i}{RT}\right), \qquad (3)$$

where A_i is the appropriate pre-exponential factor and E_i is the relevant reaction barrier. In order to minimize the number of free parameters in our model we assume that $A_{ER} = A_{LH} = A_{Rxn}$. This assumption is valid provided that neither mechanism is sterically more favorable than the other.

Our model allows both the ER and LH mechanisms to occur simultaneously, yielding an overall rate equation for product formation given by Equation (4). As discussed in detail below we only consider the ER process for the reaction of O atoms from the gas phase reacting with an adsorbed alkene (Alk) molecule:

$$r = \frac{d[\text{Product}]}{dt} = (k_{ER}[\text{Alk}]_S F_0 + k_{LH}[\text{Alk}]_S [O]_S). \qquad (4)$$

The above rate equation assumes that the reaction product does not react further with O atoms or O_2. We confirmed this assumption by irradiating a layer of product molecules (e.g., ethylene oxide and acetaldehyde) on the surface with O/O_2. No further chemistry of the product molecules was observed.

To determine the yield of product, to compare with experiment, we integrate the above equation numerically starting from the initial conditions $[O]_S = [\text{Alk}]_S = 0$ at $t = 0$. To determine the surface concentrations of the reactants and products during this integration we need to consider three processes: the desorption of the species from the surface, the consumption of the O atoms and hydrocarbons via their mutual reaction, and the deposition of the reactants onto the surface. The fluence of O atoms and the relevant alkene onto the surface can be derived from the flux of the reactants onto the surface J_i, the values of which can be estimated from the pumping speed in the target chamber and the pressure rise in the chamber due to the gases from the O atom source and the alkene, respectively. It should be noted that in the case of O atoms we initially calculate a flux of

$(O + O_2)$; the flux of O can then be estimated from the measured dissociation efficiency. The desorption rate for a given species $(X = O, C_2H_4/C_3H_6)$ at a given surface temperature can readily be calculated using Equation (5). It should be noted that we do not include the desorption of the products C_2H_4O and C_3H_6O in our model since this occurs at temperatures higher than those investigated in the desorption phase. The rate of desorption of the products over the temperature range explored in our dosing experiments is therefore expected to be extremely small:

$$r_{\text{Des},X} = A_{\text{Des},X} \exp\left(\frac{E_{\text{Des},X}}{RT}\right)[X]_S. \qquad (5)$$

The pre-exponential factor for the desorption process, $A_{\text{Des},X}$ is commonly taken as the vibrational frequency of the adsorbate–surface bond. In our model we use a value of $A_{\text{Des},O}$ of 3.10×10^{12} s^{-1}, a value derived from the potential energy curve calculated (Bergeron et al. 2008) for the adsorption of O atoms at a bridge site of pyrene. For A_{Des,C_2H_4} we use a value of 2.42×10^{12} s^{-1} (Rubes et al. 2010). Unfortunately, to our knowledge, no value of A for the adsorption of C_2H_4 on a graphite surface is available, and so we have assumed the value of A_{Des,C_2H_4} also governs the desorption of C_3H_6 ($A_{\text{Des},C_3H_6} = A_{\text{Des},C_2H_4}$). It should be noted that in our experiments we rapidly reach monolayer coverage. Consequently, for the majority of the time during our experiments, the reactants are deposited onto a multilayer ice primarily composed of alkene molecules. To our knowledge, no parameters are available in the literature describing the desorption of alkene molecules or oxygen atoms from such ices. We have therefore used the corresponding values for a graphite surface in their place. As we discuss in detail below, the desorption energies for O and C_2H_4 derived from our experiments (on multilayer alkene ices) are in very good agreement with values previously measured for a graphite surface, thus justifying our use of the desorption parameters for graphite. It should also be noted that we model the desorption of species X during the dosing process, Equation (5), as first order in the coverage of the adsorbed species. Desorption of physisorbed multilayer ices is typically found to be zero order (Burke & Brown 2010). However, in any multilayer regime, desorption of species X will just reveal another X moiety for the reaction. Hence, multilayer desorption effectively does not change $[X]_S$. Thus, only desorption in the monolayer regime will affect the rates in Equation (4). Monolayer desorption is typically first order in the surface concentration, as we model with Equation (5). The excellent fit of the numerical model to our experimental data strongly supports this analysis.

Given the above, the rate of change of the surface concentrations of the reactants is

$$\frac{d[X]_S}{dt} = -r_{\text{Des},X} - r + J_X. \qquad (6)$$

The surface concentrations of each reactant can therefore be obtained by integrating Equation (6). This then allows integration of Equation (4) to give the overall yield of the reaction product. By calculating a product yield in this manner at each of the different temperatures investigated experimentally, the dependence of the product yield on the substrate temperature is obtained.

Initially, we normalize our model yields to the experimental value of the product yield at 45 K for C_2H_4O and 50 K for C_3H_6O. Such an approach means it is not necessary to determine a value of A_{Rxn} as the temperature dependence of the modeled

yield is only dependent on the relative values of r_{LH} and r_{ER}. Thus, the normalized fit of the yields from the model to the experimental data can be used to determine E_{LH} and E_{ER}. The reaction barrier for each mechanism is then adjusted in our model until the model output fits the temperature dependence indicated by our experimental data. It should be noted that the barrier for the LH mechanism is expected to be greater than that for the ER mechanism since the former includes any barriers to the diffusion of the reactants on the surface. In addition to the reaction barriers, the normalized fit to the experimental data also allows us to extract values of the desorption energies ($E_{Des,O}$ and $E_{Des,Alk}$). The values of E_{LH} and E_{ER} critically determine the shape of the yield curve, but the values of the desorption energies only determine the relative values of the experimental yields very close to the relevant desorption temperatures. Hence, we find, via sensitivity analysis, both the reaction barriers and the desorption energies can be extracted robustly from a normalized fit to the experimental data.

To use our kinetic model to derive an absolute rate constant for these surface reactions requires placing our experimental results for C_2H_4 + O and C_3H_6 + O on an absolute scale. To achieve this objective we have determined the detection efficiency of our experimental arrangement by taking the measured total ion count of the C_nH_{2n} reactant for a given dosing/desorption experiment and dividing this number by the number of C_nH_{2n} molecules known (from $J_{C_nH_{2n}}$) to have built up on the surface during the dosing, as the number of C_2H_4 molecules consumed by the reaction with O atoms is small. This procedure is repeated at the various different surface temperatures and the results are averaged to give the proportionality constant α between the overall number of molecules present and the number of ions detected. We then use α, and the ion counts of C_2H_4O and C_2H_6O, to provide an estimate of the number of product molecules present on the surface at the end of the reaction. It should be noted that this procedure assumes the electron ionization cross sections of the reactants and products are identical. Such an assumption is unavoidable because, to our knowledge, no measurements of these electron ionization cross sections are available.

The above procedure places the experimental results on an absolute scale: number of molecules formed against surface temperature during dosing. The output of the model is also in these units and can be fitted to the experimental data, using the reaction barriers and desorption energies obtained above, by adjusting A_{Rxn}.

5. DISCUSSION

5.1. C_2H_4 + O

Fitting our experimental data with the kinetic model described above allows us to determine reaction barriers for both the ER and the LH pathways. The temperature dependence of the product yield, predicted by the kinetic model, can be seen overlaid on our experimental results in Figure 2. It is clear that there is excellent agreement between our experimental results and the predictions of the model. The values for the reaction barriers that we obtain from the fit are $E_{ER}/R = 70 \pm 15$ K and $E_{LH}/R = 190 \pm 45$ K. These barriers compare with an experimental gas-phase barrier equivalent to 974 ± 48 K (Atkinson & Cvetanov 1972). The fit to the experimental data also, as discussed above, allows the determination of the desorption energies, giving, in temperature units (E_{Des}/R) 2016 ± 12 K for C_2H_4 and 1455 ± 72 K for O atoms (16.8 kJ mol^{-1} and 12.1 kJ mol^{-1}, respectively).

The desorption energy for ethene is in excellent agreement with recently recorded, but as yet unpublished, data (2155 K) from another surface science group (M. C. Whelan & W. A. Brown 2011, private communication). Note that the uncertainty in the desorption energy of the O atom is significantly larger than that for C_2H_4 since, at the desorption temperature of O (45 K), this energy only affects the product yield from the LH mechanism which only contributes 40% of the total product yield at 45 K. Conversely, varying the desorption temperature of C_2H_4 has a much larger effect on the product yield at 70 K and so it is possible to determine this value more precisely. As discussed above, it is possible to extract the desorption energies from the fit to our experimental data, while still allowing the reaction barriers to be determined, since the desorption energies only affect the model output at specific temperatures. The data cannot therefore be fitted with an incorrect reaction barrier by manipulating the desorption energies.

Comparison of our desorption energies with interaction energies reported in the literature indicates that our values agree well with previous work. For example, the interaction energy between C_2H_4 and coronene (hollow site) is calculated to be 17.4 kJ mol^{-1}, equivalent to 2088 K (Rubes et al. 2010) and the interaction energy between O atoms and pyrene (bridge site) is calculated to be 11.6 kJ mol^{-1} (Bergeron et al. 2008), equivalent to 1395 K. These calculated values agree well with those we extract from our data. Caution should be exercised in interpreting our experimental desorption energies as simple values for adsorption on a graphite substrate. This caveat is necessary as, in the later stages of the dosing, it is expected that a layer of largely C_2H_4 ice will have built up on top of the graphite surface. However, one would expect the desorption energies of the reactants on the carbonaceous alkene ice to be broadly similar to the desorption energies on graphite, in accord with the values we extract from the kinetic model.

Additionally, again as described above, a fit to the absolute values of the product yield results in a value of A_{Rxn} of $(1.6 \pm 0.3) \times 10^{-15}$ cm^2 molecule^{-1} s^{-1}. At 15 K the value of k_{LH}, derived from A_{Rxn} and E_{LH}/R, is 5.0×10^{-21} cm^2 molecule^{-1} s^{-1}. The value of k_{ER} at 15 K, 1.5×10^{-17} cm^2 molecule^{-1} s^{-1}, is considerably larger, but is perhaps of less astrophysical relevance since surface reactions in the ISM are considered to be dominated by the LH mechanism due to the low surface coverages (Awad et al. 2005). The two rate constants are broadly comparable with rate constants extracted from studies of other astrophysically important surface reactions (Awad et al. 2005)

As mentioned above, to fit the experimental data we require only an LH channel and the ER reaction of an O atom from the gas phase with an adsorbed C_2H_4 molecule. That is, we do not include an ER reaction involving a gas-phase C_2H_4 species and an adsorbed O atom. The neglect of this second ER channel, and the good fit to the experimental data when it is neglected, can be justified since this ER reaction can only happen below 40 K, the desorption temperature of the O atom. However, at such low temperatures both species will stick and the LH mechanism is therefore likely to be much more significant than any small contribution from this ER pathway.

It can be seen from Figure 2 that the modeling indicates that the double peak in our experimental product yields is real, and is a consequence of the ER and LH mechanisms both contributing to the product yield. In Figure 2, the modeled yields from the LH and ER reactions are indicated separately. The product yield from the ER mechanism increases with temperature up to 60 K, as the rate constant increases with temperature, before

Table 1
The reaction barriers, E_a, reaction pre-exponential factors, A_{rxn}, and desorption energies, E_{Des}, estimated for
the surface reactions of O atoms with C_2H_4 and C_3H_6

Reaction	(E_a/R) (K)	A_{rxn} (10^{-15} cm^2 molecule^{-1} s^{-1})	$(E_{Des,O}/R)$ (K)	$(E_{Des,C_nH_{2n}}/R)$ (K)	k_{rxn} (cm^2 molecule^{-1} s^{-1}, at 20 K)
C_2H_4(ads) + O(ads)	190 ± 45	1.6 ± 0.3	1455 ± 72	2016 ± 12	1.20E−19
C_2H_4(ads) + O(g)	70 ± 15				4.80E−17
C_3H_6(ads) + O(ads)	145 ± 10	4.8 ± 0.4		2580 ± 4	3.40E−18
C_3H_6(ads) + O(g)	40 ± 5				6.50E−16

Note. Rate constants for the reactions studied, k_{rxn}, have also been calculated for a surface temperature of 20 K. See the text for details.

decreasing rapidly above 60 K. Since the ER reaction we consider (see above) involves the O atoms as the gas-phase species, the desorption energy of O atoms has no influence upon the product yield from the ER mechanism. However, above 60 K the lifetime of C_2H_4 on the surface decreases rapidly leading to a lower concentration on the surface and thus reduced reaction rates. Consequently, the product yield from the ER mechanism decreases rapidly above 60 K.

The contribution to the product yield from the LH mechanism, on the other hand, is critically dependent upon the desorption energy for O atoms and the associated reaction barrier. It should be noted that the barrier for the LH mechanism is somewhat larger than that for the ER mechanism. As discussed above, this is to be expected as the LH barrier, as formulated, incorporates any energy barriers to the diffusion of species on the surface; such barriers are not involved in the ER mechanism. The result of the larger barrier for the LH mechanism and the lower desorption energy for O atoms is that in the laboratory the LH mechanism only contributes to the product yield at surface temperatures between 30 and 50 K. Below 30 K the reactants are too immobile on the surface to encounter each other on a laboratory timescale, whereas above 50 K the O atoms have a very short lifetime on the surface and consequently desorb before they have time to react via the LH mechanism. The peak in the overall model output at 45 K arises from the opportunity, under our experimental time frame, for the LH mechanism to contribute to the product yield around this temperature. For easy reference, the kinetic parameters we derive for this system are summarized in Table 1.

5.2. C_3H_6 + O

The output of the kinetic model for the O + C_3H_6 reaction can be overlaid upon our experimental results (Figure 3). As was the case for the C_2H_4 + O reaction, it is again clear that there is excellent agreement between the output of the model and our experimental results. From the fit we extract reaction barriers equivalent to (40 ± 5) K for the ER reaction and (145 ± 10) K for the LH mechanism. The finding that both values are lower than those for ethene is perhaps not surprising since both reactions likely proceeds via RHC–CH$_2$O (where R = H or CH$_3$) intermediates. Such intermediates contain an electron-deficient carbon atom which can be stabilized by electron-releasing groups. The reduced barrier for the C_3H_6 + O reaction can therefore be explained by the fact that the electron-releasing methyl group present in propene can stabilize the reaction intermediate. For comparison the gas-phase reaction barrier for the O + propene reaction has been reported to be equivalent to 517 ± 48 K (Atkinson & Cvetanov 1972).

From the resolved contributions to the product yield from the ER and the LH mechanism (Figure 3) it can be seen that the ER mechanism alone can be used to fit all the data points, with the exception of the point at 40 K. The contribution of the

LH mechanism between 30 and 50 K readily accounts for the increased yield at 40 K. Satisfyingly, the excellent fit to the O + C_3H_6 data involves the same desorption energy for the O atoms as used for modeling the C_2H_4 + O reaction. The desorption energy we extract for C_3H_6 is 21.45 ± 0.03 kJ mol^{-1} (2580 K). As would be expected, this desorption energy is slightly larger than the desorption energy we determined for the lighter ethene molecule. For the O + C_3H_6 reaction, a fit to the absolute values of the product yield, as described above, results in a value of A_{Rxn} of (4.8 ± 0.4) × 10^{-15} cm^2 molecule^{-1} s^{-1}. Again, the kinetic parameters we derive for this system are summarized in Table 1.

6. ASTROPHYSICAL IMPLICATIONS

Our experimental results show that, on an analogue of an interstellar dust grain and at temperatures mimicking those in interstellar clouds, oxygen atoms can readily add to carbon–carbon double bonds to produce epoxide rings. The reaction of O atoms with C_2H_4 is detectable above a surface temperature of 12 K, with the reaction's efficiency peaking between 30 K and 50 K. In this latter regime, the reaction is highly efficient with of the order of 50% of the incident O atoms reacting to form C_2H_4O. At a surface temperature of 20 K this efficiency is reduced to approximately 5%. The reaction with propene is markedly more efficient, both at 12 K and in the 30–50 K regime. These observations indicate that thermal processing of alkene molecules by O atoms is viable in the ISM, contrary to some earlier discussion (Turner & Apponi 2001). Indeed, extrapolating our results indicates that the thermal processing of longer chain alkenes by oxygen atoms should be highly efficient under the conditions pertaining in dense interstellar clouds. The previous neglect of these thermal reactions of adsorbed oxygen atoms is due to the large barriers of the equivalent reactions in the gas phase. These large gas-phase barriers had been thought to indicate that the surface reactions would also have barriers that precluded them from occurring in interstellar environments, without the intervention of cosmic rays or UV radiation. In actual fact, the reaction barriers we determine for the C_2H_4 + O and the C_3H_6 + O reactions on our model dust grain surface are far smaller than the gas-phase values. These small barriers result in the oxygen addition reactions occurring readily between surface species thermalized at temperatures relevant to the ISM.

The major product of the surface reaction of O + C_2H_4 is ethylene oxide, a saturated molecule which is commonly considered unreactive with respect to further processing by reactive atoms on interstellar surfaces (Charnley 2004); although chemists would consider ethylene oxide potentially highly reactive due to the inherent ring strain present in the molecule. Indeed, this potential reactivity has prompted an investigation

of the ion–molecule chemistry of ethylene oxide as a potential route to pre-biotic species (Jackson et al. 2007).

By analogy with our results for O + C_2H_4, we propose that the reaction of O with C_3H_6 yields propylene oxide, but of course this product may readily isomerize to propanal or even acetone. To date, propylene oxide has not been detected in the ISM (Cunningham et al. 2007). Gas-phase isomerization of this epoxide to the more stable propanal appears to require significant activation in the gas phase (Elango et al. 2010), but may be promoted on grain surfaces by non-thermal routes. Propanal has been detected in the ISM and its formation via reactions on grain surfaces has been proposed (Hollis et al. 2004).

Astrophysical pathways for the processing of small hydrocarbons, by reactive atoms on surfaces, to form ethanol have been proposed (Charnley 2004). This scheme involves the three isomers of C_2H_4O. The inclusion in such schemes of an efficient reaction of O atoms with C_2H_4, to form predominantly ethylene oxide, would reduce the efficiency of transforming acetylene to ethanol, the net transformation considered.

We estimate our experiments to simulate the equivalent of about 10^5–10^6 years of exposure to O atoms, of the order of the lifetime of a typical molecular cloud. Thus, the transformation of ethene to ethylene oxide in these environments is eminently practical. Ethene is thought to be formed in ices as a secondary product of charged particle irradiation and photolysis of methane ices (Bennett et al. 2006). However, ethene does not appear to be a major component of interstellar ice and is likely present at unobservable concentrations of less than 1% in interstellar ice mantles (Bennett et al. 2005). Despite its low abundance in ices, non-thermal routes for the formation of the isomers of C_2H_4O from ethene have been proposed and investigated in detail experimentally (Bennett et al. 2005). These experiments, which involved the irradiation of CO/C_2H_4 ices, with the consequent reaction of O atoms with the alkene molecule, observed efficient formation of acetaldehyde and ethylene oxide, with vinyl alcohol a minor product. Coupled with the observed efficacy of irradiation of CO_2/methane ices, which yields only acetaldehyde of the C_2H_4O isomers, these non-thermal studies could rationalize the interstellar excess of acetaldehyde over ethylene oxide (Ikeda et al. 2001; Nummelin et al. 1998). However, Bennett et al. note that there would be expected to be a strong temperature dependence on the formation routes, and hence the abundances, of the C_2H_4O isomers if thermalized oxygen atoms react with ethene to yield these species (Bennett et al. 2005). Our experiments show that thermal reaction of O atoms with alkenes do indeed occur and can provide additional, temperature-dependent routes to interstellar epoxides, such as ethylene oxide, and, if appropriate isomerization pathways are available, to aldehydes. Indeed, our results indicate that in more quiescent and shielded regions, where one might expect the contribution of non-thermal pathways to be reduced, one might expect a higher relative abundance of epoxides with respect to aldehydes.

The experiments of Bennett et al. (2005) indicated that given the astronomical observation of an abundance ratio (Turner & Apponi 2001) of ethylene oxide to vinyl alcohol of 1.5, a viable route for the interstellar formation of vinyl alcohol was required, given the low branching to form this molecule in their irradiation experiments. Our laser ionization experiments show no evidence of vinyl alcohol as a major product from thermal reaction of O atoms with C_2H_4. Thus, it does not appear that thermal surface chemistry can account for the observed abundance of vinyl alcohol. It may be that, in our experiments, any vinyl alcohol formed tautomerizes to acetaldehyde when the surface is warmed in the desorption phase. However, given the low desorption temperatures observed in our experiments this seems unlikely. An alternative explanation may be that there is a substantial barrier to forming vinyl alcohol on the surface. This barrier would be more readily surmounted by energetic O atoms than by thermalized O atoms.

7. CONCLUSIONS

Using dosing on a graphite surface, monitored by temperature-programmed desorption, we reveal that both C_2H_4O and C_3H_6O are readily formed from reactions of ethene and propene molecules with thermalized oxygen atoms at temperatures in the range of 12–90 K. It is clear from these experiments that the reactions on a graphite surface proceed with significantly reduced reaction barriers compared with those for the gas-phase reaction. Indeed, for both the C_2H_4 + O and the C_3H_6 + O reactions, the surface reaction barriers we determine are reduced by approximately an order of magnitude compared with the barriers in the gas phase. The modeling of our experimental results, which determines these reaction barriers, also extracts desorption energies and rate coefficients for the title reactions. Our results clearly show that the major product from the O + C_2H_4 reaction is ethylene oxide, an epoxide.

These experiments show that thermal heterogeneous pathways can contribute to the formation of the C_2H_4O isomers in interstellar clouds. The contribution of these pathways to epoxide formation, in comparison to non-thermal routes, is likely to be strongly temperature dependent. Our results indicate an increased relative abundance of epoxides, relative to the corresponding aldehydes, could be an observational signature of a significant contribution from thermal O atom reactions with alkenes.

REFERENCES

Adriaens, D. A., Goumans, T. P. M., Catlow, C. R. A., & Brown, W. A. 2010, J. Phys. Chem. C, 114, 1892
Atkinson, R., & Cvetanov, R. J. 1972, J. Chem. Phys., 56, 432
Atkinson, R., & Pitts, J. N. 1974, Chem. Phys. Lett., 27, 467
Awad, Z., Chigai, T., Kimura, Y., Shalabiea, O. M., & Yamamoto, T. 2005, ApJ, 626, 262
Bell, M. B., Matthews, H. E., & Feldman, P. A. 1983, A&A, 127, 420
Bennett, C. J., Jamieson, C. S., Osamura, Y., & Kaiser, R. I. 2006, ApJ, 653, 792
Bennett, C. J., Osamura, Y., Lebar, M. D., & Kaiser, R. I. 2005, ApJ, 634, 698
Bergeron, H., Rougeau, N., Sidis, V., et al. 2008, J. Phys. Chem. A, 112, 11921
Bernstein, L. S., & Lynch, D. K. 2009, ApJ, 704, 226
Burke, D. J., & Brown, W. A. 2010, Phys. Chem. Chem. Phys., 12, 5947
Charnley, S. B. 2004, in Space Life Sciences: Steps toward Origin(s) of Life, ed. M. P. Bernstein, M. Kress, & R. NavarroGonzalez (Kidlington: Pergamon-Elsevier Science Ltd.), 23
Cunningham, M. R., Jones, P. A., Godfrey, P. D., et al. 2007, MNRAS, 376, 1201
Cuppen, H. M., & Herbst, E. 2007, ApJ, 668, 294
Dickens, J. E., Irvine, W. M., Ohishi, M., et al. 1997, ApJ, 489, 753
Elango, M., Maciel, G. S., Palazzetti, F., Lombardi, A., & Aquilanti, V. 2010, J. Phys. Chem. A, 114, 9864
Ferrante, R. F., Moore, M. H., Spiliotis, M. M., & Hudson, R. L. 2008, ApJ, 684, 1210
Fourikis, N., Sinclair, M. W., Robinson, B. J., Godfrey, P. D., & Brown, R. D 1974, Aust. J. Phys., 27, 425
Garozzo, M., Fulvio, D., Kanuchova, Z., Palumbo, M. E., & Strazzulla, G. 2010, A&A, 509, 9
Garozzo, M., La Rosa, L., Kanuchova, Z., et al. 2011, A&A, 528, A118
Harris, J., & Kasemo, B. 1981, Surf. Sci., 105, L281
Hartquist, T. W. (ed.) 1990, Molecular Astrophysics (Cambridge: Cambridge Univ. Press)

Hawkins, M., & Andrews, L. 1983, J. Am. Chem. Soc., 105, 2523
Herbst, E. 1995, Annu. Rev. Phys. Chem., 46, 27
Herbst, E., Roueff, E., & Talbi, D. 2010, Mol. Phys., 108, 2171
Hiraoka, K., Miyagoshi, T., Takayama, T., Yamamoto, K., & Kihara, Y. 1998, ApJ, 498, 710
Hollis, J. M., Jewell, P. R., Lovas, F. J., Remijan, A., & Mollendal, H. 2004, ApJ, 610, L21
Hudson, R. L., & Moore, M. H. 1997, Icarus, 126, 233
Hudson, R. L., & Moore, M. H. 2003, ApJ, 586, L107
Ikeda, M., Ohishi, M., Nummelin, A., et al. 2001, ApJ, 560, 792
Islam, F., Latimer, E. R., & Price, S. D. 2007, J. Chem. Phys., 127, 064701
Jackson, D. M., Adams, N. G., & Babcock, L. M. 2007, J. Am. Soc. Mass Spectrom., 18, 445
Kaiser, R. I., & Roessler, K. 1998, ApJ, 503, 959
Knyazev, V. D., Arutyunov, V. S., & Vedeneev, V. I. 1992, Int. J. Chem. Kinet., 24, 545
Latimer, E. R., Islam, F., & Price, S. D. 2008, Chem. Phys. Lett., 455, 174
Lattelais, M., Pauzat, F., Ellinger, Y., & Ceccarelli, C. 2010, A&A, 519, 7
Lias, S. G. 2011, in NIST Chemistry WebBook, NIST Standard Reference Database Number 69, ed. P. J. Linstrom & W. G. Mallard (Gaithersburg, MD: National Institute of Standards and Technology)
Marcelino, N., Cernicharo, J., Agúndez, M., et al. 2007, ApJ, 665, L127

Matthews, H. E., Friberg, P., & Irvine, W. M. 1985, ApJ, 290, 609
Nummelin, A., Dickens, J. E., Bergman, P., et al. 1998, A&A, 337, 275
Perry, J. S. A., Gingell, J. M., Newson, K. A., et al. 2002, Meas. Sci. Technol., 13, 1414
Perry, R. A. 1984, J. Chem. Phys., 80, 153
Rubes, M., Kysilka, J., Nachtigall, P., & Bludsky, O. 2010, Phys. Chem. Chem. Phys., 12, 6438
Schriver, A., Schriver-Mazzuoli, L., Ehrenfreund, P., & d'Hendecourt, L. 2007, Chem. Phys., 334, 128
Snow, T. P., & McCall, B. J. 2006, ARA&A, 44, 367
Stuhl, F., & Niki, H. 1971, J. Chem. Phys., 55, 3954
Tielens, A. G. G. M. 2005, The Physics and Chemistry of the Interstellar Medium (1st ed.; Cambridge: Cambridge Univ. Press)
Turner, B. E. 1991, ApJS, 76, 617
Turner, B. E., & Apponi, A. J. 2001, ApJ, 561, L207
Turner, B. E., Terzieva, R., & Herbst, E. 1999, ApJ, 518, 699
Ung, A. Y. M. 1975, Chem. Phys. Lett., 32, 351
Williams, D. A., & Hartquist, T. W. 1999, Acc. Chem. Res., 32, 334
Williams, D. A., & Herbst, E. 2002, Surf. Sci., 500, 823
Wise, H., & Wood, B. J. 1967, Adv. At. Mol. Phys., 3, 291
Ziurys, L. M., & McGonagle, D. 1993, ApJS, 89, 155